

06,13

Microstructure of spherulitic lead zirconate titanate thin films

© M.V. Staritsyn¹, V.P. Pronin², I.I. Khinich², S.V. Senkevich³, E.Yu. Kaptelov³,
I.P. Pronin³, A.S. Elshin⁴, E.D. Mishina⁴

¹ NRC „Kurchatov Institute“ — CRISM „Prometey“,
St. Petersburg, Russia

² Herzen State Pedagogical University of Russia,
St. Petersburg, Russia

³ Ioffe Institute,
St. Petersburg, Russia

⁴ MIREA — Russian Technological University,
Moscow, Russia

✉ E-mail: Pronin.v.p@yandex.ru

Received July 4, 2023

Revised July 4, 2023

Accepted July 5, 2023

The features of the microstructure of radiant spherulites in lead zirconate titanate thin films are studied using scanning electron and nonlinear optical microscopy by varying the blocks size of the perovskite structure. It is shown that as the spherulite radius (or block size) increases, the rotation angle of the growth axis increases, the rotation angle velocity changes, and the magnitude of the second optical harmonic signal changes.

Keywords: Lead zirconate titanate thin films, PZT, scanning electron microscopy, nonlinear optical microscopy, pyrochlore-perovskite phase transformation.

DOI: 10.61011/PSS.2023.08.56577.140

1. Introduction

There has been a boom in research of materials used in microelectromechanical systems (MEMS) of various functional purposes in the world in the last decade. A large share in these applications is played by devices based on thin-film ferroelectrics, characterized by high values of electromechanical parameters. The primacy among ferroelectrics belongs to solid solutions of lead zirconate titanate (PZT), in which abnormally high electromechanical coefficients are observed in the region of the morphotropic phase boundary (MPB) separating rhombohedral and tetragonal modifications of the ferroelectric phase [1–3]. The values of these coefficients are significantly affected by the technological parameters of the formation of thin films, the presence of foreign impurities and phases, the heterogeneity of their composition, microstructure, mechanical stresses acting from the substrate and the sublayers used, as well as a number of other factors [4–6]. The competitiveness of PZT films is determined both by the efficiency of the technologies used for their formation, high electromechanical coefficients, and the presence of natural unipolarity (self-polarization), when its magnitude is commensurate with the magnitude of spontaneous polarization of the material [6–8].

Silicon (Si) substrate, which is still the basis of modern microelectronics, is widely used for the formation of capacitor thin-film PZT structures, while not being optimal for the MEMS production. The integral temperature coefficient of linear expansion of silicon is less than the same value

for the PZT film, the composition of which corresponds to MPB. This leads to the fact that in the operating temperature range, two-dimensional tensile mechanical stresses act on the film from the substrate side, partially reorienting the vector of spontaneous polarization in the direction as close as possible to the plane of the film [7,9,10]. This reduces both the magnitude of self-polarization and the stability of the macroscopic polar state. The magnitude of self-polarization also depends on the mechanism of crystallization of the perovskite phase, the presence of excess lead oxide and its localization in the volume of a thin film [11].

Another factor influencing the structure and physical properties of thin films is the mechanisms of the formation of the perovskite phase of thin films, which differ either in the layered or insular character of growth [12]. Practice has shown that the crystallization of thin polycrystalline films occurs with the formation and proliferation of the island structure when silicon substrates are used [13–15]. For the most part, perovskite islands are characterized by a shape close to round, and comprise spherulitic formations which grow either through a step-ring mechanism, or with the formation of a radial-radiant structure [13,16,17].

It is well known that spherulitic structures are widespread in nature, inherent in various kinds of organic and inorganic materials. In particular, spherulites are widely represented in minerals in the form of balls of radially radiant structure, for which they received the name of radiant spherulites [18,19]. In thin-film materials, radiant spherulites are similar in shape to disks, the radius of which can reach several tens

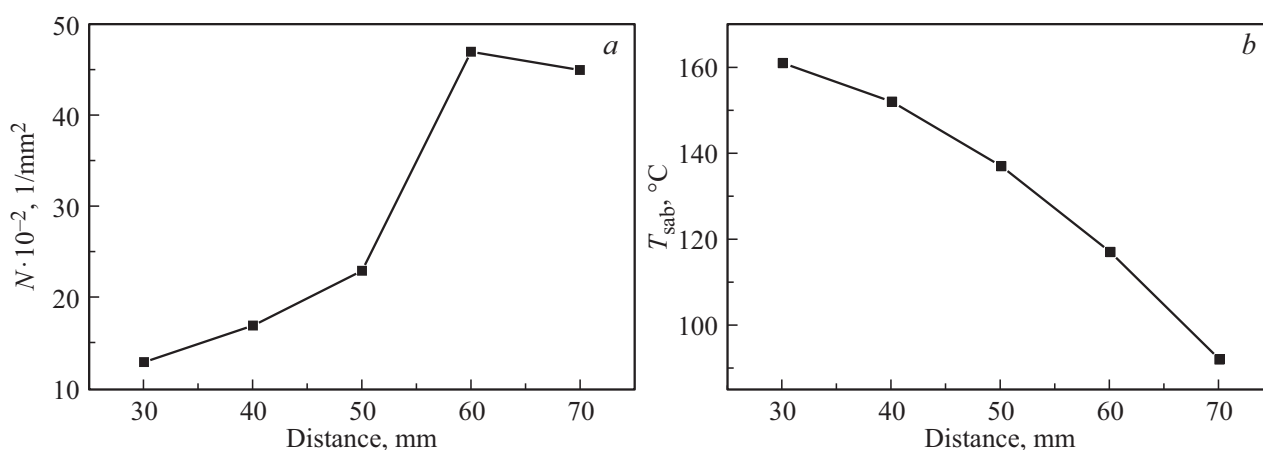


Figure 1. Change in the concentration of nucleation centers (a) and substrate temperature during deposition (b) with varying target–substrate distance.

or even hundreds of micrometers. The recent interest in „two-dimensional“ spherulites, their microstructure and properties is mainly related to the development of miniature piezoelectric quartz oscillators, for the manufacture of which thin-film technologies must be used. One of the characteristic features of the crystallization of quartz radiant spherulites from the amorphous phase is the rotation of their growth axis during their radial expansion. During the subsequent merger of spherulitic islands, a block spherulitic microstructure with linear boundaries [20,21] is usually formed.

The very early studies of thin PZT films carried out in the 90s of the last century found that the crystallization of the perovskite phase is also accompanied by the formation of radiant spherulites. Most studies of thin films were carried out with linear dimensions of spherulites not exceeding several micrometers in diameter based on the assumption that the radiant spherulite is a rather complex crystalline formation, in which local structural and physical properties may differ in area. Apparently, therefore, the properties of both spherulite islands and single-phase films with a pronounced spherulite structure have not been studied until now. In this paper, the task was to investigate the microstructure features of perovskite thin films with a change in the concentration of the centers of formation of spherulite islands, leading to a change in the average size of spherulite blocks.

2. Preparation of thin film specimens and study methods

Thin films with a thickness of ~ 500 nm were produced by the two-stage RF magnetron deposition [15]. The sprayed ceramic target of the PZT corresponded to the stoichiometric composition $\text{PbZr}_{0.54}\text{Ti}_{0.46}\text{O}_3$ related to the MPB region. The temperature of the subsequent high-temperature annealing (T_{ann}) was $\sim 550^{\circ}\text{C}$ to obtain island

films, and was $\sim 580^{\circ}\text{C}$ to obtain single-phase perovskite films. The change of the concentration of the crystallization centers of the perovskite phase was achieved by changing the distance from the target to the substrate in the range 30–70 mm, resulting in a change in the temperature of heating the substrate with gas plasma (T_{sub}) [22,23], Fig. 1, a, b.

The crystal structure and phase state of the films were controlled by X-ray diffraction analysis (Rigaku Ultima IV) and optical microscopy (Nikon Eclipse LV150). The microstructure of the spherulitic structure was studied using scanning electron microscopy (SEM) (Zeiss EVO-40 and Tescan Lyra 3) in the modes of backscattered electrons and electrons backscattered diffraction.

The second optical harmonic was excited by the radiation of a femtosecond laser with a wavelength of 800 nm, a repetition frequency of 80 MHz and a duration of 100 fs. The intensity of the generation of the second optical harmonic (SHG) was recorded at a wavelength of 400 nm. The plane of polarization of the incident beam was rotated by a half-wave plate in front of the specimen. The Glan prism was used as an analyzer. The images were fixed in the geometry „on reflection“. Zeiss N-achroplan 100X lens of the WITec alpha 300S confocal microscope provided a spot on a specimen with a diameter of $0.9\ \mu\text{m}$, and the use of optical fiber ensured a spatial resolution of ~ 300 nm.

3. Experimental results and discussion

Fig. 2 shows images of spherulite islands obtained in the mode of back-reflected electrons (Fig. 2, a) and using nonlinear optical microscopy (SHG signal) (Fig. 2, b, c). The perovskite islands were characterized by a radially radiant structure, clearly observed on both SEM and SHG images. A strong difference in the SHG signal is apparent between the inner and outer regions of the islands, as evidenced by the distribution of the SHG signal along the diametral

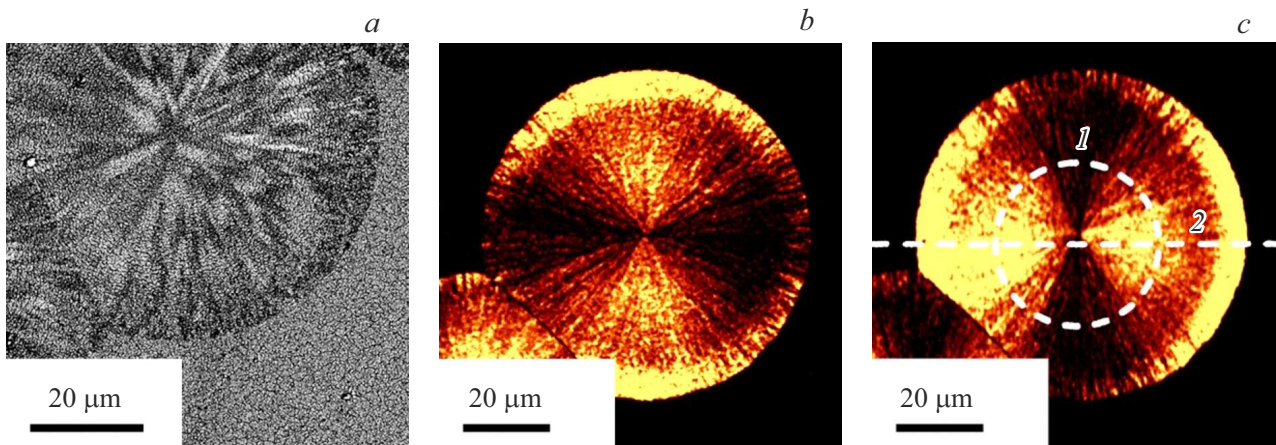


Figure 2. SEM (a) and nonlinear optical images (b,c) of perovskite islands in a pyrochlore matrix. The maps of the SHG signal (b and c) differ by changing the orientation of linearly polarized radiation by 90 degrees. Dotted lines on (c) mark diametrical and circular sections (1,2).

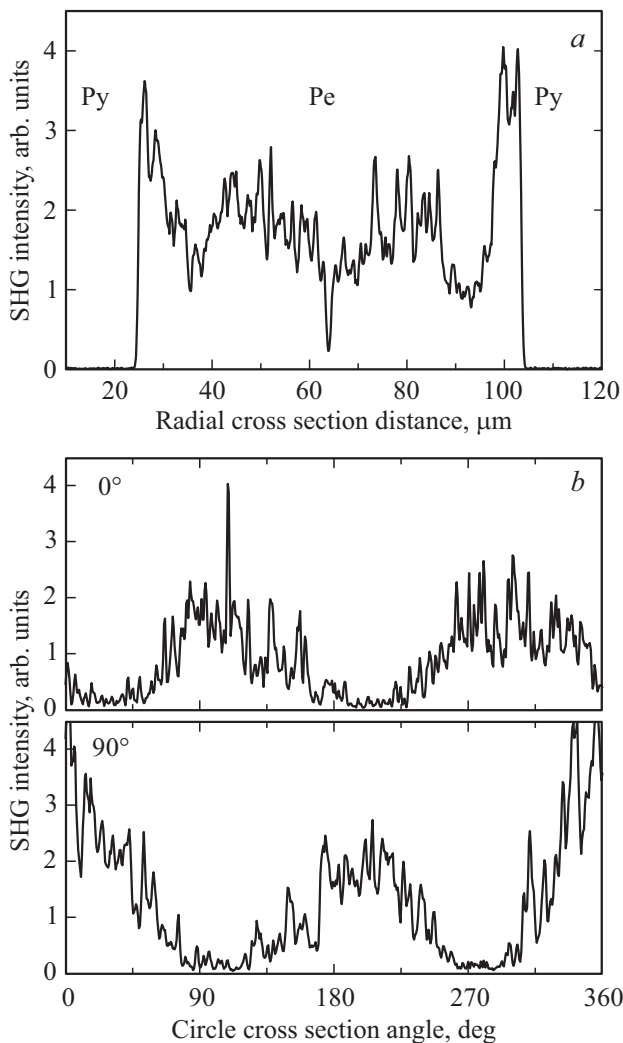


Figure 3. Distribution of the SHG signal a) by section 1 (Fig. 2, c) of the spherulite island, b) along the circular cross section 2 (Fig. 2, c) of the spherulite island and when the polarization of the incident beam is rotated by 90°.

(radial) section of the spherulite (Fig. 3, a, section 1 in Fig. 2, c). The SHG signal in the center of the island is close to zero. This signal increases moving away from the center of the spherulite reaching a local maximum approximately at the middle of the radius, then it decreases to the edge and increases again at a distance of $\sim 5-7 \mu\text{m}$ to the edge. The magnitude of the SHG signal at the periphery of the spherulites increases by ~ 2 times compared to the signal in the central region. This behavior may indicate a two-stage formation of the perovskite phase from the pyrochlore phase: first, the crystallization of the „of the loose“ phase of perovskite, and then its recrystallization into a denser modification [15]. Earlier, we assumed that the amplification of the SHG signal at the edges (periphery) of the islands is associated with the relaxation of mechanical stresses in the marginal regions [23]. However, the results obtained in this work indicate rather the presence of another mechanism for increasing the signal.

Circular cross-section of the SHG signal in a spherulitic island (cross-section 2 in Fig. 2, c) with a fixed direction of polarization has two maxima and two minima close to zero (Fig. 3, b). When the polarization of the incident radiation is rotated, the distribution of the SHG signal along the circular section rotates by the same angle. This behavior can be observed if the polarization component lying in the plane of the film is oriented in the radial direction in a spherulite consisting of multiple radial crystallites (growing from a single crystallization center).

Fig. 4, a, d, g shows maps of the crystallographic orientations of the growth axes relative to the normal to the surface in continuous perovskite films of PZT consisting of separate spherulitic blocks. The films were deposited at different substrate temperatures (T_{sub}) and then annealed at 580°C. The maps were obtained by recording the diffraction of backscattered electrons. The red, green and blue colors correspond to the growth axes $\langle 100 \rangle$, $\langle 110 \rangle$ and $\langle 111 \rangle$. Intermediate positions correspond to other colors on

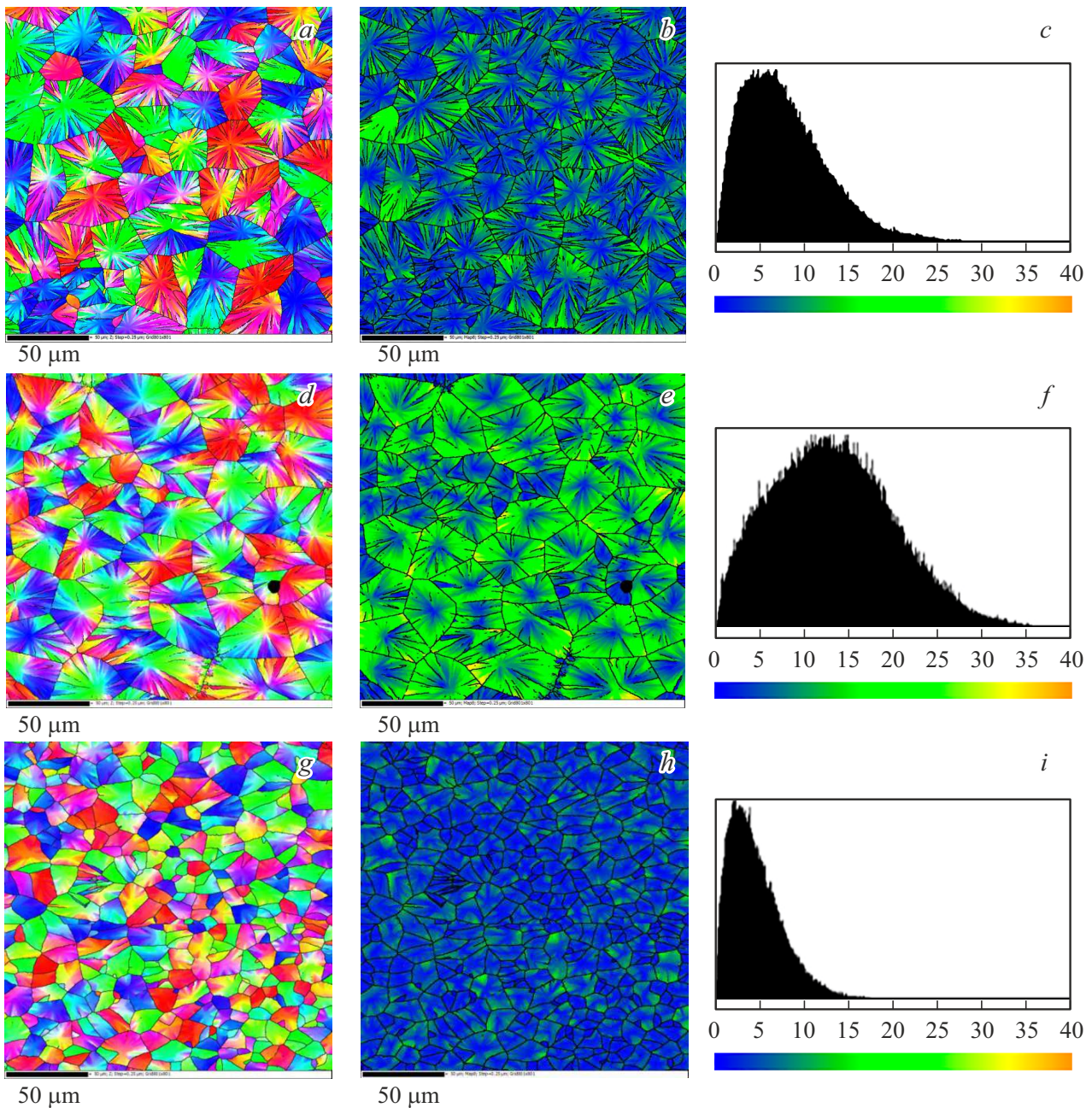


Figure 4. Maps of the crystallographic orientations of the growth axes (*a, d, g*), maps of the distribution of the angles of intrablock deviations (*b, e, h*) and their histograms of the distribution by the magnitude of the deviation from the average orientation (*c, f, i*).

the maps of crystallographic orientation. The average block size increases significantly with an increase in the substrate temperature T_{sub} , at which films were deposited — from 10–15 μm at $T_{\text{sub}} = 90^\circ\text{C}$ to 40–45 μm at $T_{\text{sub}} = 160^\circ\text{C}$. In addition, in films deposited at $T_{\text{sub}} = 160^\circ\text{C}$, additional open radially located large-angle boundaries with misorientation of at least 10 degrees were observed within each of the blocks, representing transition layers with crystalline disturbances.

Fig. 4, *b, e, h* shows maps of the distribution of angles of deviations of the growth axes from the average orientation

in each spherulitic block. The average orientation of the block corresponds to deep blue, pronounced deviations are colored by green. The increase of these deviations is mainly correlated with the increase of the size of spherulitic blocks. The distributions of deviation angles are shown in the form of histograms on Fig. 4, *c, f, i*.

Figure 5 shows the dependence of the magnitude of the mean-angle deviations when the target-substrate distance changes. As the average size of spherulitic blocks increases, an increase in this value is observed, however, in films deposited at $T_{\text{sub}} = 160^\circ\text{C}$, a sharp drop in this value occurs,

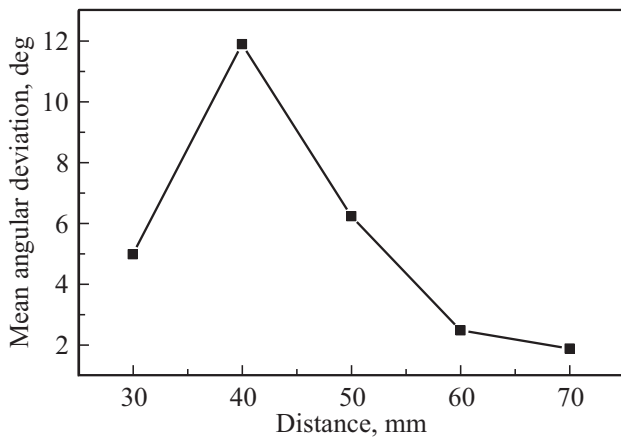


Figure 5. The angle averaged on the map of intrablock deviations of the orientations of the growth axis from the average direction when the target-substrate distance changes.

which is noticeably reflected on the map of the distribution of deviation angles (Fig. 4, *h*).

Fig. 6 demonstrates the change of the angle of rotation of the growth axis as the radial distance from the center of the spherulite (along the dotted line in Fig. 6, *a*). Studies showed that this dependence is mainly linear in nature (Fig. 6, *b*). Comparison with the data obtained for quartz spherulites ($0.5\text{--}0.7\text{ grad}/\mu\text{m}$) [20,21] shows that in perovskite spherulites the rotation speed reaches somewhat higher values. The rate of angle change in the studied specimens increases with T_{sub} , reaches a maximum ($1.2\text{ grad}/\mu\text{m}$) at $T_{\text{sub}} = 150^\circ\text{C}$, and then decreases sharply, Fig. 7. The nature of the change of the rotation speed correlates with the average value of intrablock deviations of growth orientations.

An abnormally strong change in the SHG signal was observed when the size of the spherulites changed (Fig. 8). The SHG signal was small in films deposited at low

substrate temperatures, but the signal value increased approximately 20 times with an increase of T_{sub} and reached a maximum at $T_{\text{sub}} = 150^\circ\text{C}$, and then sharply decreased. Since the SHG signal is proportional to the square of the polarization projection lying in the plane of the film, its change means a change in the polarization value by $\sim 3\text{--}3.5$ times.

The interpretation of the results obtained is associated with the assumption that with the increase in the linear dimensions of spherulitic blocks, mechanical stresses increase in the plane of the thin film. The appearance of mechanical stresses with the island nature of the nucleation and growth of the perovskite phase from the low-temperature pyrochlore phase is associated with a change in the density of these phases. The data of X-ray diffraction studies showed that the density of the Pe phase is 7–8% higher than the density of the pyrochlore phase. Partial relaxation of the resulting mechanical stresses occurs through shrinkage of the perovskite phase (at 3–5%). In this regard, the perovskite phase is formed, as a rule, in two stages: at the first stage, the an intermediate porous („loose“) perovskite structure is formed, and at the second, the loose phase turns into its denser modification [15,23]. This is also evidenced by the presence of a periphery (Fig. 2), different from the central part of the spherulite, and an abnormal change in the signal of the SHG (Fig. 3, *a*).

The rotation of the polarization of the incident light radiation, which leads to a 90-degree extinction of the SHG signal (Fig. 4, *b, c*), confirms the assumption about the radial nature of the orientation of ferroelectric polarization. It should be noted that since the studied composition of thin films corresponds to the region of the morphotropic phase boundary, where the free energies of rhombohedral, monoclinic and tetragonal phases are close to each other [24], the reorientation of spontaneous polarization under the action of tensile forces in the radial direction should be greatly facilitated. The increase of the SHG signal with an increase in the linear dimensions of spherulitic

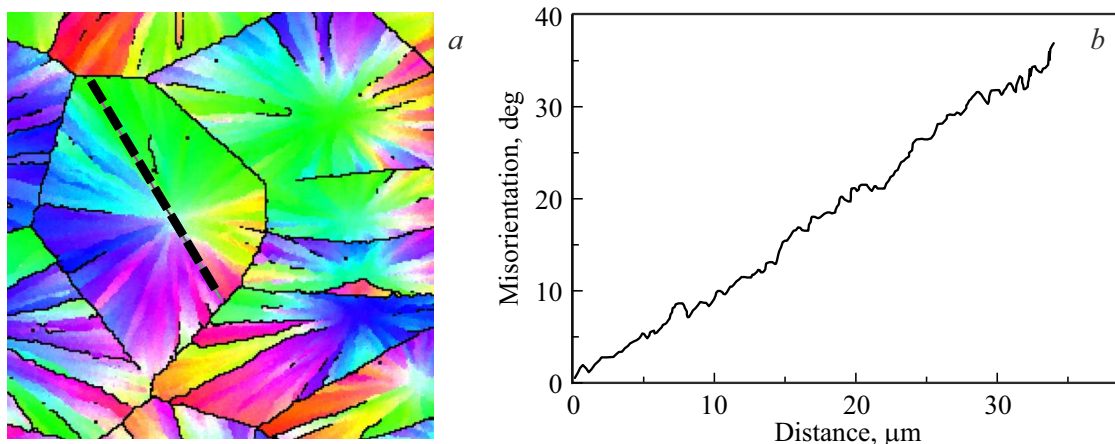


Figure 6. A map of the crystallographic orientations of the growth axes relative to the normal to the surface (*a*) and the angle of rotation of the growth axis (*b*) along the dotted line shown in Fig. 6, *a*.

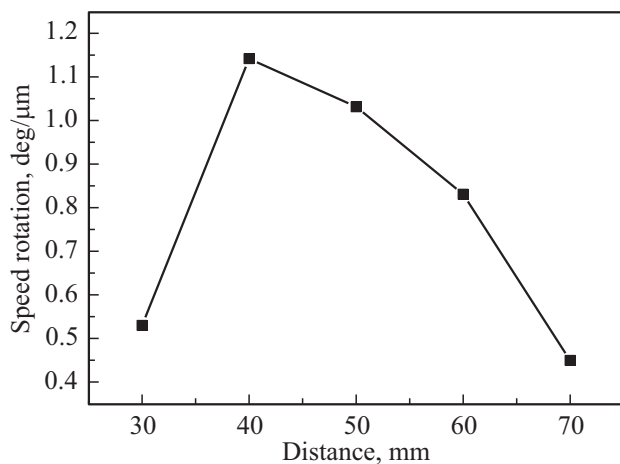


Figure 7. The rotation speed of the growth axis when the distance of the target–substrate change.

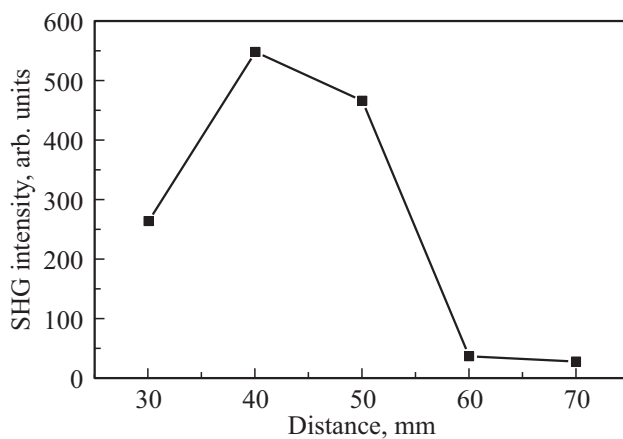


Figure 8. Change of the signal intensity of the second optical harmonic when the distance of the target–substrate changes.

blocks is apparently caused not only by the reorientation of ferroelectric polarization in the direction collinear (or antiparallel) to mechanical stresses radially stretching the spherulite, but also by an increase in the induced component of polarization under the influence of these stresses.

Such features as a two-fold decrease in the signal of the SHG in the film (formed at $T_{\text{sub}} = 160^\circ\text{C}$) while maintaining large spherulitic blocks, a decrease in the rotation speed of the growth axis, a decrease in intrablock deviations of the growth axes and the appearance of large-angle boundaries in spherulitic blocks may indicate that such boundaries arise as a result of relaxation of strong mechanical stresses reaching the threshold values of the destruction of the material. The upper threshold of these stresses is estimated as $\sim 0.1 E_Y$ (E_Y — Young's modulus, which is for thin films of PZT ~ 110 GPa, according to [25]) and can reach a value of ~ 11 GPa. The induced ferroelectric polarization is estimated at $100 \mu\text{C}/\text{cm}^2$ at these tensile mechanical stresses and the magnitude of the piezoelectric module $\sim 90 \cdot 10^{-12}$ C/N [25].

4. Conclusion

Two-phase (island) and single-phase thin PZT films characterized by a radiant spherulite microstructure with the composition of corresponding to the MPB region were grown in this paper. The films had different concentrations of nucleation centers (or linear sizes differing in 3–4 times). It was found that:

- the change in the microstructure and the SHG signal from the center to the periphery in island radiant spherulites is caused by the recrystallization of the perovskite phase and the formation of a radiant microstructure,

- the rotation of the growth axis was observed in spherulitic blocks at a speed of $0.5\text{--}1.2$ grad/ μm , depending on the linear size of the spherulites,

- it is assumed that the observed effects such as: changes in the microstructure of the blocks, the signal of the SHG, the rotation speed of the growth axes and other characteristics defined in the work are caused by the action of mechanical stresses in the plane of thin films, the magnitude of which increases with the increase of the size of spherulitic blocks. Mechanical stresses are caused by a change in the phase density during the crystallization of thin PZT films, and new large-angle boundaries are formed in the result of relaxation of mechanical stresses,

- the action of mechanical stresses leads to the orientation of the lateral component of polarization in the radial direction.

It is planned to further study the polar properties of thin PZT films using piezoelectric response force microscopy to gain a better understanding of the impact of mechanical stresses in radiant spherulites on the orientation of polarization.

Funding

The study was supported by an internal grant of the Herzen State Pedagogical University of Russia, No. 25 VN. Experimental studies were carried out using the equipment provided by the Center for the Collective Use of Scientific Equipment „Composition, Structure and Properties of Structural and Functional Materials“ National Research Center „Kurchatov Institute“ — Central Research Institute of Structural Materials „Prometey“.

Conflict of interest

The authors declare that they have no conflict of interest.

References

- [1] B. Jaffe, W. Cook, H. Jaffe. Piezoelectric ceramics. London; N.Y.: Academic Press, (1971). 328 p.
- [2] D.L. Polla. Microelectron. Eng. **29**, 51 (1995).
- [3] L. Song, S. Glinsek, E. Defay. Appl. Phys. Rev. **8**, 041315 (2021).

- [4] N. Izyumskaya, Y.-I. Alivov, S.-J. Cho, H. Morko, H. Lee, Y.S. Kang. *Critic. Rev.Solid State Mater. Sci.* **32**, 3, 111–202 (2007).
- [5] Y. Ma, J. Song, X. Wang, Y. Liu, J. Zhou. *Coatings* **11**, 8, 944 (2021).
- [6] A.L. Kholkin, K.G. Brooks, D.V. Taylor, S. Hiboux, N. Setter. *Integr. Ferroelectrics* **22**, 525 (1998).
- [7] R. Bruchhaus, D. Pitzer, M. Schreiter, W. Wersing. *J. Electroceram.* **3**, 151 (1999).
- [8] V.P. Afanasjev, A.A. Petrov, I.P. Pronin, E.A. Tarakanov, E.Ju. Kaptelov, J. Graul. *J. Phys.: Condens. Matter* **13**, 39, 8755 (2001).
- [9] T. Ogawa, A. Senda, T. Kasanami. *JJAP* **30**, 9S, 2145 (1991).
- [10] I.P. Pronin, E.Yu. Kaptelov, A.V. Goltsev, V.P. Afanasyev. *Phys. Sol. St.* **45**, 9, 1768 (2003).
- [11] V.V. Osipov, D.A. Kiselev, E.Yu. Kaptelov, S.V. Senkevich, I.P. Pronin. *Phys. Sol. St.* **45**, 9, 1768 (2003).
- [12] Yu.I. Yuzyuk, I.N. Zakharchenko, V.A. Aleshin, I.N. Leontiev, L.M. Rabkin, V.M. Mukhortov, P. Simon. *Phys. Sol. St.* **49**, 9, 1759 (2007).
- [13] G.A.C. Spierings, J.B.A. Van Zon, P.K. Larsen, M. Klee. *Integr. Ferroelectrics* **3**, 283 (1993).
- [14] V.Ya. Shur, E.B. Blankova, A.L. Subbotin, E.A. Borisova, A.V. Barannikov. *Phys. Sol. St.* **43**, 5, 902 (2001).
- [15] V.P. Pronin, S.V. Senkevich, E.Yu. Kaptelov, I.P. Pronin. *Poverkhnost'. J. Surf. Investig.*, **4**, 5, 703 (2010).
- [16] I. Bretos, R. Jimenez, M. Tomczyk, E. Rodriguez-Castellon, P.M. Vilarinho, M.L. Calzada. *Sci. Rep.* **6**, 20143 (2016).
- [17] V.P. Pronin, D.M. Dolgintsev, V.V. Osipov, I.P. Pronin, S.V. Senkevich, E.Yu. Kaptelov. *IOP Conf. Series: Mater. Sci. Eng.* **387**, 012063 (2018).
- [18] B.Z. Cantor. *Besedy o mineralakh. Astrel, M.* (1997). 216 p. (in Russian).
- [19] A.G. Shtukenberg, Y.O. Punin, E. Gunn, B. Kahr. *Chem. Rev.* **112**, 3, 1805 (2012).
- [20] N.R. Lutjes, S. Zhou, J. Antoja-Lleonart, B. Noheda, V. Ocelík. *Sci. Rep.* **11**, 1, 14888 (2021).
- [21] E.J. Musterman, V. Dierolf, H. Jain. *Intern. J. Appl. Glass Sci.* **13**, 3, 402 (2022).
- [22] M.V. Staritsyn, M.L. Fedoseev, D.A. Kiselev, E.Yu. Kaptelov, I.P. Pronin, S.V. Senkevich, V.P. Pronin. *Phys. Sol. St.* **65**, 2, 290 (2023).
- [23] A.S. Elshin, I.P. Pronin, S.V. Senkevich, E.D. Mishina. *Tech. Phys. Lett.* **46**, 4, 385 (2020).
- [24] D.E. Cox, B. Noheda, G. Shirane. *Phys. Rev. B* **71**, 134110 (2005).
- [25] H. Nazeer, M.D. Nguyen, Ö.S. Sukas, G. Rijnders, L. Abelman, M.C. Elwenspoek. *J. Microelectromech. Syst.* **24**, 1, 166 (2015).

Translated by A.Akhtyamov